

ON THE INTERGRANULAR HYDROGEN EMBRITTLEMENT MECHANISM OF Al-Li ALLOYS

T. I. Zohdi and E. I. Meletis

Department of Mechanical Engineering
Louisiana State University, Baton Rouge, Louisiana 70803

(Received February 11, 1992)
(Revised March 16, 1992)

Introduction

The presence of hydrogen can cause embrittlement in a wide variety of materials ranging from conventional materials to advanced alloys, intermetallics and ceramics. Hydrogen can be introduced in materials in the atomic form (H) either electrolytically or from a gaseous atmosphere. Hydrogen - induced embrittlement results in subcritical crack growth at loading levels significantly lower than those associated with unstable crack motion. Two major proposals exist with regard to the hydrogen embrittlement (HE) mechanism. The first model advocates that HE is due to hydrogen-induced decohesion that occurs at the highest stress triaxility region [1,2]. The second proposal is based on a hydrogen-induced microplasticity mechanism occurring in front of the crack tip [3,4]. It is evident that the region in the immediate vicinity of the crack tip is of utmost importance since this is where the critical stress field environment (hydrogen) interaction occurs, leading to embrittlement and crack propagation. In the presence of a crack, H penetration in front of the crack tip can occur mainly by stress assisted diffusion and dislocation transport. It has been recently shown that hydrogen is a key element in the embrittlement of Al-Li alloys [5]. Because of the very high atomistic hydrogen mobility at the grain boundaries, grain boundary diffusion is expected to play a crucial role in the intergranular embrittlement of Al-Li alloys. The purpose of this paper is to investigate the stress assisted grain boundary diffusion of H in Al-Li alloys in an effort to shed light on the intergranular embrittlement mechanism.

Experimental Observations

Commercial 2090 Al alloy (Al-2.2Li-2.9Cu-0.12Zr) in the T8 condition was used in the experimental study. The material was produced in the form of a rolled plate, and its microstructure consisted of flattened grains with average dimensions $1100\mu\text{m} \times 240\mu\text{m} \times 11\mu\text{m}$. Double cantilever beam (DCB) specimens were prepared from the plate in the SL orientation, which is the most sensitive orientation since the crack plane lies parallel to the flattened grain boundaries. The DCB specimens were 2.54 cm high (plate thickness), 1.3 cm wide and 12.5cm long, providing valid plane strain conditions. The specimen was first fatigue precracked to develop a sharp and straight crack front and subsequently tested in 3.5% NaCl solution (pH=6.9) under cathodic charging (-1500 mV vs. SCE) by loading at a constant $K_I = 8.62\text{ MPa}^{\frac{1}{2}}$, which corresponds to Stage II cracking.

The crack growth measurements showed that the crack advances in a discontinuous mode with a consistent overall crack velocity (Stage II) of about $5 \times 10^{-8}\text{ m/s}$. SEM examinations of the fracture

surfaces showed an exclusively intergranular cracking mode. Cracking occurs on parallel but displaced grain boundaries separated by unfractured ligaments. Failure of the ligaments produces "river patterns" on the fracture surface. Detailed fracture surface observation revealed the presence of two types of crack - arrest markings (CAM): micro - and macro - CAM. The micro-CAM indicate the position of individual crack jumps, and their average spacing for a $K_I = 8.62 MPa m^{1/2}$ was determined to be about $30 \mu m$. Both types of CAM run perpendicular to the direction of the crack propagation and had a curved appearance due to plane stress conditions prevailing at the specimen surfaces. Measurements of the spacing between macro- CAM showed that they corresponded to the jump events monitored on the specimen surface. Thus, the measured velocity reflects the overall crack velocity that relates to the ligament fracture and not to the velocity of the individual jumps. It is evident that, as the crack advances, the length of the unfractured ligaments increases and exercises a continuously stronger restraining effect on the stress intensity acting at the crack tip. Eventually, the stress intensity is decreased below the threshold value (K_{th}), and the crack is arrested [6].

The crack front resides at these sites (macro - CAM) until the ligaments are fractured by stress environment interactions and the crack propagation process resumes. Thus, under intergranular HE, the ligament fracture seems to be the slowest step and controls the overall crack velocity. Regarding the individual crack jump velocity, it is expected to be significantly faster, and an estimate is made in a later section.

Hydrogen Diffusion Under Stress Free Conditions

The hydrogen transport modes in metals and alloys are mainly of two types, i.e., diffusion under a concentration gradient and transport by moving dislocations. In the stress free case, the diffusion mode is the only transport process. Fisher's model [7] was used as the basis to describe the diffusion process along the grain boundary (along the x axis) and in the lattice of the present material. The grain boundary thickness is δ and is assumed to be so thin that concentration variations across its width are negligible. Effectively, the instantaneous concentration in the slab (grain boundary) is a function of x only. The hydrogen concentration in the slab then varies according to the equation

$$\frac{\partial C_{gb}}{\partial t} = D_{gb} \frac{\partial^2 C_{gb}}{\partial x^2} + D_l \left(\frac{2}{\delta} \frac{\partial C_l}{\partial y} \right)_0 \quad |y| < \frac{\delta}{2} \quad (1)$$

where C is the hydrogen concentration, D is the hydrogen diffusivity and gb and l denote grain boundary and lattice, respectively. The first term represents the concentration change associated with diffusion of hydrogen along the slab, and the second term the diffusion (along the y axis) from the two sides of the slab into the lattice [7]. Note that the last term is evaluated at the grain boundary.

The continuity requirements at the edge of the grain boundary need C_l and C_{gb} to be in equilibrium. In this case, the segregation of hydrogen at the grain boundary is related to C_l according to the following equation [8]

$$C_{gb} = C_l \exp\left(\frac{\Delta G}{kT}\right) = C_l K_{eq} \quad (2)$$

where ΔG is the binding free energy between a hydrogen atom and the grain boundary. The coefficient of C_l is the segregation factor, K_{eq} , and will vary with temperature (T) in an exponential manner. Therefore, the equation for diffusion in the grain boundary can be rewritten as

$$\frac{\partial C_{gb}}{\partial t} = D_{gb} \frac{\partial^2 C_{gb}}{\partial x^2} + D_l \left(\frac{2}{\delta K_{eq}} \frac{\partial C_{gb}}{\partial y} \right)_0 \quad |y| < \frac{\delta}{2} \quad (3)$$

This last term on the right is typically quite small [8] and can be omitted; it essentially states that the concentration in the grain boundary depends only on the diffusion down the grain boundary. The diffusion out of the grain boundary, while significant to the concentration in the lattice, is not significant to the grain boundary.

Hydrogen Diffusion Under Stress Assisted Conditions

In the presence of a crack, accelerated H penetration is anticipated in the region in front of the crack tip by stress - assisted diffusion and dislocation transport. Our previous results [9] have shown that very little plastic deformation is involved in the intergranular cracking of the test material. Therefore, H transport by dislocations is not expected to contribute significantly in the accumulation of H in front of the crack tip and is not considered in the present study.

Van Leeuwen's equation [10] can be used to describe the diffusion of hydrogen in the presence of a stress field

$$\frac{\partial C_{gb}}{\partial t} = D_{gb} \frac{\partial C_{gb}^2}{\partial^2 x} - \frac{D_{gb} V_H}{RT} \frac{\partial \sigma}{\partial x} \frac{\partial C_{gb}}{\partial x} \quad (4)$$

V_H is the partial molar volume of hydrogen and R is the gas constant. For plane strain and assuming a perfectly elastic - plastic solid with no work hardening, we may use Hill's slip line field equation for the hydrostatic stress in the plastic zone (σ_p) immediately ahead of a blunted crack of radius ρ given by [11]

$$\sigma_p = \sigma_y \left[\ln \left(1 + \frac{x}{\rho} \right) + \frac{1}{2} \right] \quad (5)$$

where σ_y is the material's yield strength (307 MPa) and x is the distance ahead of the crack tip. The distribution of hydrostatic stress in the elastic region may be assumed, for simplicity, to be given by the solution for a sharp crack [12]

$$\sigma_e = \frac{2}{3} (1 + \nu) \frac{K_I}{(2\pi x)^{\frac{1}{2}}} \quad (6)$$

where ν is Poisson's ratio (0.3 for this alloy) and K_I is the apparent applied stress intensity ($8.6 \text{ MPa}^{\frac{1}{2}}$). Also, the plastic zone size r_p in front of the crack tip can be calculated from

$$r_p = \frac{(1 - 2\nu)^2 K_I^2}{2\pi \sigma_y^2} \quad (7)$$

For the present test material and loading conditions, it is estimated that $r_p = 21 \mu\text{m}$. Using this r_p value and knowing that the hydrostatic stress at the plastic and elastic zones must be equal at this distance, one can determine the crack tip radius to be $5.3 \mu\text{m}$. The resulting hydrostatic stress distribution ahead of a notch is shown in Figure 1.

The steady state solute concentration $C(x)$, at any point, x, within the stress field is given by [13, 14]

$$C(x) = C_0 \exp \left(\frac{\sigma_i V_H}{3RT} \right) \quad (8)$$

where σ_i is the summation of the principle stresses such that $\frac{\sigma_i}{3}$ is the hydrostatic component of the applied stresses. C_0 is the concentration at the surface of the crack tip without stress, and $C_s = C(x = 0)$ will be the concentration at the surface after loading. The equilibrium concentration profiles for hydrogen in the plastic [11] and elastic [15] regimes are given by

$$\text{plastic} \quad C(x) = C_0 \exp\left[\frac{V_H}{RT} \sigma_y \left(\ln\left[1 + \frac{x}{\rho}\right] + \frac{1}{2}\right)\right] \quad x < r_p \quad (9)$$

$$\text{elastic} \quad C(x) = C_0 \exp\left[\frac{V_H}{RT} \frac{2}{3} (1 + \nu) \frac{K_I}{(2\pi x)^{\frac{1}{2}}}\right] \quad x > r_p \quad (10)$$

For the present alloy the steady state hydrogen concentration (at r_p) is shown in Figure 2. The maximum concentration is reached at r_p and is equal to $1.8C_0$.

It is reasonable to assume that the crack will advance when a critical hydrogen concentration (C_c) is obtained in front of or at the crack tip, and the particular combination of stress and hydrogen concentration is sufficient to produce cracking. Assuming an elastic - perfectly plastic material, the stress distribution indicates that the stress level is maximum at r_p , and from Van Leeuwen's equation it is expected that the hydrogen concentration will reach the critical level first at r_p , the edge of the plastic zone. Thus, the incremental crack nucleates at the edge of the plastic zone and extends towards the tip of the original crack. It should be noted that the incremental crack has sufficient energy and can also propagate forwards in the region which is stressed above a critical hydrostatic stress level (σ_c) and has relatively high H concentration. The σ_c is interpreted as the stress at C_c achieved at $t = \infty$ when the K_{th} is applied at the crack. By using the model developed by Doig and Jones [16], one can calculate the σ_c from the equation:

$$K_{th} = \frac{3\sigma_c}{2(1 + \nu)} [2\pi\rho \left(\exp\left(\frac{\sigma_c}{\sigma_y} - \frac{1}{2}\right) - 1\right)]^{\frac{1}{2}} \quad (11)$$

By assuming a K_{th} of $5.2 \text{ MPa m}^{\frac{1}{2}}$, one can calculate the critical stress (σ_c) to be 517.5 MPa whereas the peak stress (at r_p) was found to be 645 MPa .

From the stress distribution, it is evident that the elastic stress remains higher than σ_c for approximately $12 \mu\text{m}$ in front of r_p , where H concentration is expected to be at relatively high levels. This shows that the individual crack jump Δx can be as long as $33 \mu\text{m}$ ($r_p + 12 \mu\text{m}$), which is in excellent agreement with the experimental evidence. Furthermore, by slightly modifying the model by Doig and Jones, one can obtain the time Δt between subsequent crack events by using the equation:

$$1 - \text{erf}\left[\frac{r_p}{2(D_{gb}\Delta t)^{\frac{1}{2}}}\right] = \exp\left(\frac{V_H}{RT} [\sigma_c - \sigma_{p,e}]\right) \quad (12)$$

where $\sigma_{p,e}$ is the hydrostatic stress at the edge of the plastic zone and $\sigma_{p,e} = \sigma_p = \sigma_e$. By using the above equation, and assuming $D_{gb} = 2.2 \times 10^{-10} \text{ m}^2/\text{s}$ [8] and $V_H = 3 \times 10^{-6} \text{ m}^3/\text{mole}$ [17], we determined that $\Delta t = 32 \text{ s}$. This time interval produces an individual crack jump velocity of 10^{-6} m/s . This velocity is about one and a half orders of magnitude higher than the overall crack velocity ($5 \times 10^{-8} \text{ m/s}$), and agrees with the notion that the slowest step in the crack propagation process is the ligament fracture.

With the time to initiation for a crack known, the transient concentration profile of hydrogen was determined by solving Van Leeuwen's equation numerically with Finite Difference, applying the following boundary conditions: $C(x = L) = 0$ and $C(x = 0) = C_0 \exp\left(\frac{\sigma_0 V_H}{2RT}\right)$, where L is the specimen length. Figure 2 shows the steady state concentration profile for stress assisted diffusion, and the transient concentration at the initiation time (32 s) for both stress assisted diffusion and stress free diffusion. It is evident that the presence of the stress field not only promotes H diffusion but also changes the H concentration profile. The maximum H concentration occurs in the vicinity of r_p (and converges to that point at steady state), and furthermore there is a significant H in the region just in front of r_p (where $\sigma_e < \sigma_c$) justifying the points made previously regarding the forward direction of the crack jump.

Conclusions

In summary, based on experimental observations and theoretical predictions, we present the view that the intergranular hydrogen embrittlement process involves the nucleation of an incremental crack at the edge of the plastic zone that extends backwards and joins the original crack but also forwards in the region that is stressed above a critical stress level and has a relatively high hydrogen concentration. Our predictions of the crack jump distance are in excellent agreement with the experimental observations. The velocity of the individual crack jumps was estimated to be about one and a half orders of magnitude higher than the overall crack velocity that was experimentally observed, showing that ligament fracture is the step controlling the hydrogen embrittlement fracture process.

References

1. A.R. Troiano, Trans. ASM 52, 54(1960).
2. R.A. Oriani, Ber. Bunse. Phyz. Chem. 76, 301(1972).
3. C.D. Beachem, Metall. Trans. 3, 437(1972).
4. H.K. Birnbaum, Environment-Sensitive Fracture of Engineering Materials, Ed. Z.A. Foroulis, p.326, TMS-AIME(1979).
5. E.I. Meletis and W.Huang, Mat. Sci. Eng. A 148, 197(1991).
6. E.I. Meletis and E. C. Aifantis, Scripta Met. et Mat. 25, 847(1991).
7. J.C. Fisher, J. Appl. Phys. 22, 74(1951).
8. W. Huang, MS Thesis, Louisiana State University, 1990.
9. E.I. Meletis, Mat. Sci. Eng. 93, 235(1987).
10. H.P. Van Leeuwen, Corrosion 29, 197(1973).
11. W. W. Gerberich and Y. T. Chen, Metall. Trans. A 6A, 271(1975).
12. H. W. Liu, J. Basic Engng. ASME 92, 633(1970).
13. R. A. Oriani, Fundamental Aspects of Stress Corrosion Cracking, p.32, NACE, Houston(1969).
14. W. W. Gerberich and C. E. Hartbower, ibid. p.420.
15. C. St. John and W. W. Gerberich, Metall. Trans. 4, 589(1973).
16. P. Doig and G.T. Jones, Metall. Trans. 8A, 1993(1977).
17. W. Beck, P. K. Subramanyan and F. S. Williams, Corrosion 27, 115(1971).

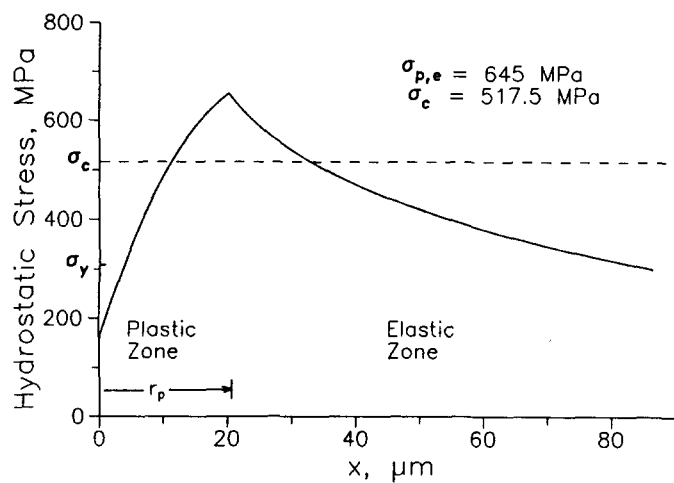


Figure 1: Schematic of the crack and the resulting stress distribution.

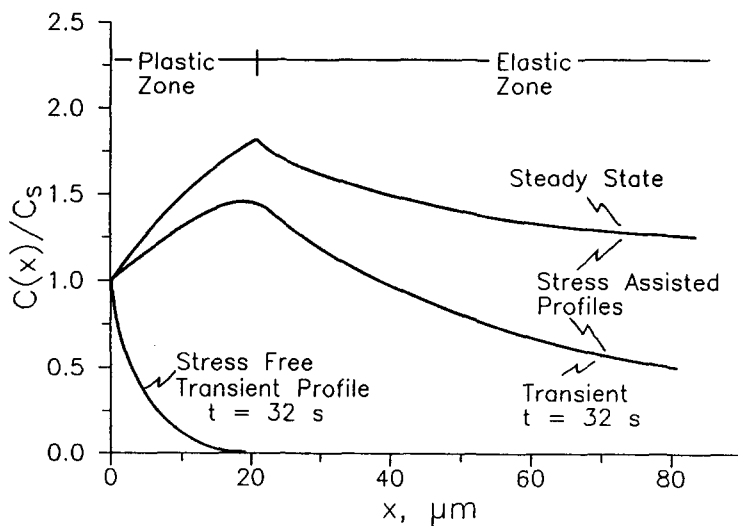


Figure 2: Transient hydrogen concentration profiles of stress free and stressed conditions at $\Delta t = 32\text{ s}$ and steady state profile under stress assisted diffusion.